

# Multiple Light Sources and Reflectance Property Estimation based on a Mixture of Spherical Distributions

Kenji Hara

Dept. of Visual Communication Design  
Kyushu University  
hara@design.kyushu-u.ac.jp

Ko Nishino

Dept. of Computer Science  
Drexel University  
kon@cs.drexel.edu

Katsushi Ikeuchi

Dept. of Computer Science  
The University of Tokyo  
ki@cvtl.iis.u-tokyo.ac.jp

## Abstract

*In this paper, we propose a new method for simultaneously estimating the illumination of the scene and the reflectance property of the object from a single image. We assume that the illumination consists of multiple point sources and the shape of the object is known. Unlike previous methods, we will recover not only the direction and intensity of the light sources, but also the number of light sources and the specular reflection parameter of the object. First, we represent the illumination on the surface of a unit sphere as a finite mixture of von Mises-Fisher distributions by deriving a spherical specular reflection model. Next, we estimate this mixture and the number of distributions. Finally, using this result as initial estimates, we refine the estimates using the original specular reflection model. We can use the results to render the object under novel lighting conditions.*

## 1. Introduction

Recovering illumination conditions and/or surface reflectances from images is commonly referred to as *inverse rendering* which has been studied actively in computer vision and computer graphics. For instance, estimation can benefit rendering under novel illumination conditions, adding new synthetic objects, and modifying the surface reflectances. The more information about the lighting we can estimate from the images (e.g. direction, location, intensity, and color of the light sources), the wider variety of illumination manipulation can be accomplished to the original images. A variety of approaches have been proposed to estimate illumination given a single view image of a scene, most of which estimate the direction of a single light source [6]. Recently, attempts have been made to recover information of multiple light sources. Yang et al. [21] analyze the intensities and surface normals along the occluding boundaries. Zheng et al. [23] use shading information along image contours. Hougen et al. [5] solve a set of linear equations for image irradiance. Marschner et al.

[9] produce a set of basis images and find a linear combination of those basis images that matches the input image. Kim et al. [7] use image regions corresponding to bumps. Sato et al. [13] analyze intensity information inside shadows cast on the scene by the object. Zhang et al. [22] detect critical points where the surface normal is perpendicular to some light source direction. Ramamoorthis et al. [12] introduce a signal-processing framework which expresses the light field as a product of spherical harmonic coefficients of reflectance and lighting. Wang et al. [18] extend Zhang et al.'s method by allowing Lambertian objects of arbitrary known shapes. More recently, multiple cues are combined to robustly estimate multiple light sources. Wang et al. [19] develop a method based on shadows and a method based on shading independently. Li et al. [8] integrate multiple cues (shading, shadow and specular reflection). Unlike other methods, Li et al.'s technique still work for textured surfaces.

Most of these methods assume (i) all the light sources are infinitely distant (i.e., directional light sources), (ii) the geometry of the target object is known, (iii) the number of light sources is known.<sup>1</sup> In this paper, we focus on recovering the illumination, including the number of light sources, and surface reflectance even in the case where the number of light sources is not given (thereby assumption (iii) is eliminated).

We propose a new method for estimating the illumination of a scene and the reflectance property of a real object in the scene, given a single view image taken under multiple point light sources and a geometric model of the object. Unlike previous methods, our method can recover not only the direction and intensity of multiple light sources but also the number of light sources and the specular reflectance property of the object. This approach can be summarized as follows. First, using the specular reflection component separated from the input image, we represent the illumination

---

<sup>1</sup> The approaches of estimating intensities of uniformly sampled light directions are also included in this category.

condition as a finite mixture of von Mises-Fisher distributions on the unit sphere based on a spherical representation of specular reflection. Then, we estimate initial values by solving both the mixture and the number of light sources using an EM optimization framework. Finally, using the results as initial estimates, we solve an optimization problem using the original specular reflection model in Cartesian coordinates. The results allows us to render the object under novel lighting conditions.

The rest of the paper is organized as follows. Section 2 explains the von Mises-Fisher distribution defined on the surface of a sphere. Using this distribution model, we derive a spherical specular reflection model based on the Torrance-Sparrow reflection model. Section 3 explains how to represent the specular reflection as a mixture of spherical distributions, and how to formulate the illumination estimation problem as the mixture estimation problem. Next, we show how we can estimate both the parameters of each distribution and the number of components in the mixture. Section 4 shows the experimental results. Finally, we conclude in Section 5.

## 2. A Reflection Model based on Spherical Distribution

Reflection models are generally divided into the diffuse reflection component and the specular reflection component. Torrance and Sparrow [16] modeled the specular reflection at an object surface point based on the assumption that the object surface is made of highly reflective microscopic facets distributed in V-shaped grooves (called the *microfacets*) as follows:

$$\mathbf{I}_S = \int_{\Omega} \frac{\mathbf{K}_S F G}{\cos \theta_r} L_i(\theta_i, \phi_i) \exp\left[-\frac{\alpha^2}{2\sigma^2}\right] d\omega_i \quad (1)$$

where  $\mathbf{I}_S$  denotes a three band color vector of the specular reflection radiance,  $\mathbf{K}_S$  is the color vector of the specular reflection (which includes the normalization factor of the exponential function, the reflectivity of the surface, and the scaling factor between scene radiance and a pixel value),  $F$  is the Fresnel reflectance coefficient,  $G$  is the geometrical attenuation factor,  $\theta_r$  is the angle between the viewing direction and the surface normal, and  $\theta_i$  and  $\phi_i$  are, respectively, the altitude and azimuth coordinate,  $L_i(\theta_i, \phi_i)$  is the illumination radiance per unit solid angle coming from the direction  $(\theta_i, \phi_i)$ ,  $d\omega_i$  is the infinitesimal solid angle ( $d\omega_i = \sin \theta_i d\theta_i d\phi_i$ ),  $\alpha$  is the angle between the surface normal and the bisector of the viewing direction and the light source direction, and  $\sigma$  is the surface roughness.

From (1), we can clearly see that the Torrance-Sparrow reflection model approximates the distribution of the orientations of microfacets with a Gaussian distribution with mean zero and standard deviation  $\sigma$ . In this section, we de-

rive a specular reflection model based on a spherical distribution (or a directional distribution) instead of the Gaussian distribution and we present that this reflection model can well approximate the Torrance-Sparrow reflection model.

### 2.1. Von Mises-Fisher Distribution

To analyze statistically directional data, the von Mises-Fisher (hereafter referred to as vMF) distribution [4] has been developed by the analogy with the Gaussian distribution and is one of the most widely used directional distributions. A direction can be expressed by a point on a sphere of unit radius. A three dimensional unit random vector (i.e.,  $\mathbf{x} = (x_1, x_2, x_3)^T$  satisfying  $\|\mathbf{x}\| = 1$ ) is said to obey 3-variate vMF distribution if its probability density function is given by

$$f(\mathbf{x}|\boldsymbol{\mu}, \kappa) = \frac{\kappa}{4\pi \sinh \kappa} \exp[\kappa \mathbf{x}^T \boldsymbol{\mu}] \quad (2)$$

where  $\boldsymbol{\mu}$  ( $\|\boldsymbol{\mu}\| = 1$ ) is the mean direction, and  $\kappa \geq 0$  is the concentration parameter. The concentration parameter  $\kappa$  characterizes how strongly the unit vectors drawn accordingly to  $f(\mathbf{x}|\boldsymbol{\mu}, \kappa)$  are concentrated around the mean direction  $\boldsymbol{\mu}$ . Let  $\chi = \{\mathbf{x}_1, \dots, \mathbf{x}_N\}$  be a data set of  $N$  random unit vectors (a set of directions) following a vMF distribution model. Let  $\mathbf{R}$  be the vector sum of these vectors. Then, the point estimator,  $\boldsymbol{\mu}_{ML}$ , of the mean direction is obtained by simply normalizing  $\mathbf{R}$  to a unitlength. The point estimator of  $\kappa$  is given by

$$\kappa_{ML} = \frac{N-1}{N-R} \quad (3)$$

where  $R = \|\mathbf{R}\| = \sum_{i=1}^N \mathbf{x}_i^T \boldsymbol{\mu}_{ML}$ .

The density function (2) can be rewritten in terms of a spherical polar coordinate system as follows:

$$P(\theta, \phi) = \frac{\kappa}{4\pi \sinh \kappa} \exp[\kappa \cos \theta] \quad (4)$$

where  $\theta \in [0, \pi]$  and  $\phi \in [0, 2\pi]$  are the polar and azimuth angles from the mean direction, respectively.

### 2.2. The Spherical Torrance-Sparrow Model

Let  $S$  be the direction mirror-symmetric (with respect to the normal  $H$  to the microfacet) to the surface normal  $N$  (Fig. 1: Left). Then we assume that  $S$  obeys a vMF distribution with mean direction  $N$  (Fig. 1: Right). More specifically, the probability of finding a direction  $S$  within a unit angular area centered at an angle,  $(\theta, \phi)$ , from the surface normal direction  $N$  is given by (4). Now,  $\theta \in [0, \pi]$  is clearly equal to twice the angle,  $\alpha$  ( $\alpha$  in (1)), between  $N$  and  $H$ . Hence, this probability is proportional to  $\exp[-2\kappa \sin^2 \alpha]$ , since  $\exp[\kappa \cos \theta] = \exp[\kappa \cos 2\alpha] = \exp[\kappa] \exp[-2\kappa \sin^2 \alpha]$ . Similar to the derivation of the

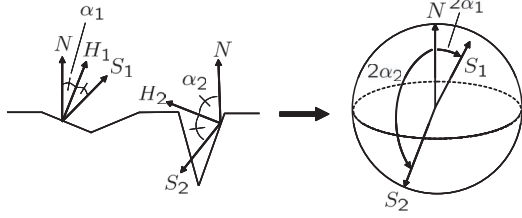


**Figure 1.** Reflection model based on spherical distribution.

Torrance-Sparrow model, we replace the exponential function on the right side of (1) with  $\exp[-2\kappa \sin^2 \alpha]$  as follows:

$$\int_{\Omega} \frac{\mathbf{K}_S F G}{\cos \theta_r} L_i(\theta_i, \phi_i) \exp[-2\kappa \sin^2 \alpha] d\omega_i \quad (5)$$

The concentration parameter  $\kappa$  here means the “smoothness” of the object surface. Also, we assume the following relation between the surface smoothness  $\kappa$  and surface roughness  $\sigma$  in such a manner that (5) is equivalent to (1) for small values of  $\alpha$  (hence,  $\sin \alpha \approx \alpha$ ).

$$\kappa = \frac{1}{4\sigma^2} \quad (6)$$

On the other hand, it is well known that the Torrance-Sparrow reflection model can be simplified by redefining  $F$  and  $G$  as constant values, under the condition that the angle between the viewing and illumination directions is smaller than  $60^\circ$  [14]. Thus, we also simplify (5) as,

$$\mathbf{I}_S = \int_{\Omega} \frac{\mathbf{K}_S}{\cos \theta_r} L_i(\theta_i, \phi_i) \exp[-2\kappa \sin^2 \alpha] d\omega_i \quad (7)$$

where  $\mathbf{K}_S$  is redefined as  $\mathbf{K}_S F G$ . We call this specular reflection model the *spherical Torrance-Sparrow reflection model*.

Fig. 2 displays the approximation of the specular reflection radiance by the spherical Torrance-Sparrow model as well as its approximation by the original Torrance-Sparrow model. From Fig. 2, we can see that these two simulation curves agree very closely with each other if  $\sigma$  may vary in  $[0, 0.2]$  (it is known that  $\sigma$  generally takes between 0.001 and 0.2) and  $\alpha$  is within  $[0, 60^\circ]$  (necessary condition for Torrance-Sparrow model simplification). This implies that the spherical Torrance-Sparrow model can be regarded as an approximation to the Torrance-Sparrow model, and hence also to the specular reflection.

### 3. Multiple Point Light Source and Reflectance Estimation

In this section, we formulate the illumination condition as a mixture of vMF distributions on the unit sphere based

on the spherical Torrance-Sparrow reflection model, and then initially estimate the illumination and specular reflectance parameters using the Expectation Maximization (EM) framework for this mixture model. The resulting estimates are then refined using a local optimization scheme based on the original Torrance-Sparrow reflection model.

#### 3.1. A Mixture Representation of Illumination Condition

We assume that the scene is illuminated by a finite number of distant point light sources (i.e., directional lights) that all have the same color. Also, the specular reflectance property of the object surface is assumed to be homogeneous.

With these assumptions, (7) can be discretely approximated using the nodes of a geodesic dome [10, 13] as

$$\mathbf{I}_S \approx \mathbf{I}_S \mathbf{L}, \quad \mathbf{I}_S = \frac{2\pi}{N_L} \frac{K_S}{\cos \theta_r} \sum_{l=1}^{M_L} L_l \exp[-2\kappa \sin^2 \alpha_l] \quad (8)$$

where  $\mathbf{L}$  is the normalized color vector with the assumption that all the light sources have the same color,  $N_L$  is the number of the nodes of a geodesic dome in a northern hemisphere,  $M_L$  is the number of the point light source,  $L_l$  ( $l = 1, \dots, M_L$ ) is the radiance of the  $l$ -th light source, and  $\alpha_l$  is the angle between the surface normal and the bisector of the viewing direction and the  $l$ -th light source direction.

Now suppose that light rays emanate in all directions from the viewing point, some of the light rays pass through the image plane toward the object and strike the object surface. Then, we map the value of  $\widetilde{I}_S = I_S \cos \theta_r = \sqrt{I_{S,R}^2 + I_{S,G}^2 + I_{S,B}^2} \cos \theta_r$  of each pixel to the mirror reflection direction at the corresponding surface point. We call the resulting scalar field on the unit sphere the *illumination sphere*.

The angle between this mirror reflection direction and the  $l$ -th light source direction is given by

$$\psi_l = \arccos(\cos(2\alpha_l) + 2 \sin^2 \alpha_l \sin^2 \theta_r \sin^2 \phi_l) \quad (9)$$

where  $\phi_l$  is the azimuth angle of the bisector of the viewing direction and the  $l$ -th light source direction from the surface normal. Since the specular reflection can be only observed when  $\alpha_l$  has very small values, we ignore the second term in (9) and approximate  $\psi_l$  as  $\psi_l \approx \arccos(\cos(2\alpha_l)) = 2\alpha_l$ . Hence, the scalar value,  $\widetilde{I}_S(\mathbf{x} | \Theta)$ , of a location,  $\mathbf{x}$ , on the illumination sphere is represented as:

$$\begin{aligned} \widetilde{I}_S(\mathbf{x} | \Theta) &= \frac{2\pi K_S}{N_L} \sum_{l=1}^{M_L} L_l \exp\left[-2\kappa \sin^2\left(\frac{1}{2} \arccos(\mathbf{x}^T \boldsymbol{\mu}_l)\right)\right] \\ &= \frac{2\pi K_S e^{-\kappa}}{N_L} \sum_{l=1}^{M_L} L_l \exp\left[\kappa \cos(\arccos(\mathbf{x}^T \boldsymbol{\mu}_l))\right] \end{aligned}$$

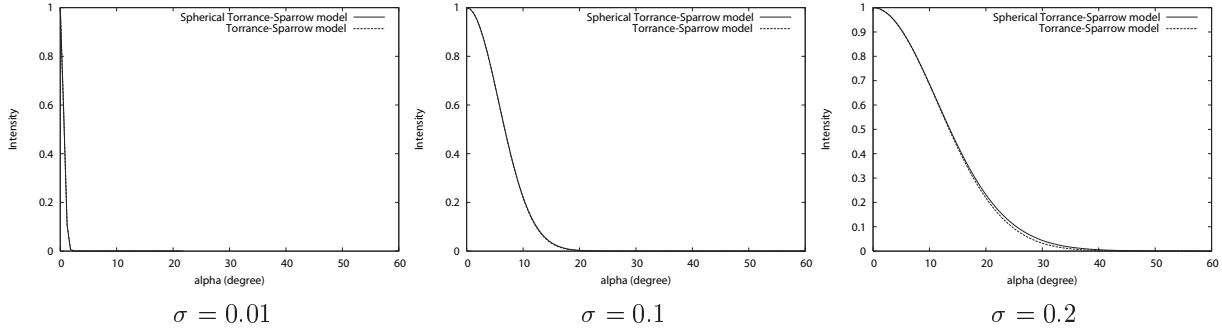


**Figure 2.** Approximation of the specular reflection radiance, for a fixed  $\sigma$ , with respect to variations of  $\alpha$ , by the spherical Torrance-Sparrow model (solid line) as well as the approximation by the original Torrance-Sparrow model (dotted line).

$$= \frac{2\pi K_S e^{-\kappa}}{N_L} \sum_{l=1}^{M_L} L_l \exp[\kappa \mathbf{x}^T \boldsymbol{\mu}_l] \quad (10)$$

where  $\boldsymbol{\mu}_l$  is the direction of the  $l$ -th light source and  $\Theta = \{L_1, \dots, L_{M_L}, \boldsymbol{\mu}_1, \dots, \boldsymbol{\mu}_{M_L}, \kappa\}$  is a set of the illumination and specular reflection parameters.

From (10), we can clearly see that the illumination sphere is equivalent to a mixture of vMF distributions, since

$$\widetilde{I}_S(\mathbf{x} | \Theta) \propto \sum_{l=1}^{M_L} L_l f(\mathbf{x} | \boldsymbol{\mu}_l, \kappa) \quad (11)$$

where  $L_l$  is redefined as the relative radiance of the  $l$ -th light source so that  $\sum_{l=1}^{M_L} L_l = 1$ , and  $f(\cdot | \boldsymbol{\mu}_l, \kappa)$  is a vMF probability density function. As a result, the mixture weight, the number of components, the mean direction and concentration parameter of each component distribution correspond to  $L_l$  (the relative radiance of the  $l$ -th light source),  $M_L$  (the number of the light source),  $\boldsymbol{\mu}_l$  (the direction of the  $l$ -th light source), and  $\kappa$  (the surface smoothness), respectively. Therefore, the problem of estimating illumination and specular reflection parameters can be formulated as a vMF mixture estimation problem with respect to  $\Theta = \{L_1, \dots, L_{M_L}, \boldsymbol{\mu}_1, \dots, \boldsymbol{\mu}_{M_L}, \kappa\}$ . However, note that, unlike usual mixture estimation, the concentration parameter (or surface smoothness)  $\kappa$  is common to all the component distributions. This corresponds to the fact that when  $\kappa$  is independently defined for each component distribution, each surface point has different reflectance properties for different light sources, which is physically nonsense. Also note, under the assumption of the original Torrance-Sparrow model, the scalar field on the sphere is expressed as a linear combination of two dimensional Gaussian distributions for data in  $\mathbf{R}^2$ , so that the illumination estimation problem cannot be treated as a mixture estimation problem.

### 3.2. EM Algorithm for Illumination Sphere

We regard the problem of simultaneously estimating the multiple point light sources and the specular reflectance as a problem of estimating a mixture of vMF distributions, as described above. To estimate the parameters of a Gaussian mixture, the Expectation Maximization (EM) algorithm is widely used for its numerical stability and simplicity.

Recently, Banerjee et al. [1] proposed two variants (called the *hard-assignment scheme*, *soft-assignment scheme*) of the EM algorithm for estimating the parameters of a mixture of vMF distributions. In this paper, we adopt Banerjee et al.'s EM algorithm for our parameter estimation problem. Note that their EM algorithm cannot be straightforwardly applied to this case, since our vMF mixture model, unlike the normal vMF mixture, includes the concentration parameter ( $\kappa$ ) which is common to all the component distributions, as mentioned before. In order to deal with this problem, we introduce the hard-assignment scheme in the E (Expectation) step and an updating rule based on the point estimator (3) in the M (Maximization) step. Also, for the parameters except  $\kappa$ , we use their soft-assignment scheme. Let  $\mathcal{X} = \{\mathbf{x}_1, \dots, \mathbf{x}_N\}$ , ( $\|\mathbf{x}_i\| = 1, \forall i$ ) a data set. Then, our EM algorithm chooses randomly  $M_L$  points (unit vectors) as the initial cluster means  $\boldsymbol{\mu}_l$  ( $l = 1, \dots, M_L$ ) and then iterates the following steps until convergence.

(1) E-step

Update the distributions of the hidden variables for  $i = 1, \dots, N$  and  $l = 1, \dots, M_L$  as:

$$p(l | \mathbf{x}_i, \Theta) \leftarrow \frac{L_l f(\mathbf{x}_i | \boldsymbol{\mu}_l, \kappa)}{\sum_{l'=1}^{M_L} L_{l'} f(\mathbf{x}_i | \boldsymbol{\mu}_{l'}, \kappa)}$$

$$q(l | \mathbf{x}_i, \Theta) \leftarrow \begin{cases} 1 & l = \operatorname{argmax}_{1 \leq l' \leq M_L} L_{l'} f(\mathbf{x}_i | \boldsymbol{\mu}_{l'}, \kappa) \\ 0 & \text{otherwise.} \end{cases}$$

(2) M-step

Update each parameter for  $l = 1, \dots, M_L$  as:

$$L_l \leftarrow \frac{1}{N} \sum_{i=1}^N p(l | \mathbf{x}_i, \Theta), \quad \boldsymbol{\mu}_l \leftarrow \frac{\sum_{i=1}^N \mathbf{x}_i p(l | \mathbf{x}_i, \Theta)}{\|\sum_{i=1}^N \mathbf{x}_i p(l | \mathbf{x}_i, \Theta)\|}$$

$$\kappa \leftarrow \frac{N-1}{N - \sum_{i=1}^N \sum_{l=1}^{M_L} q(l | \mathbf{x}_i, \Theta) \mathbf{x}_i^T \boldsymbol{\mu}_l}$$

Note that the number of component distributions is assumed to be known. Nevertheless, one of the advantages of solving this inverse rendering problem within the EM framework is that the optimal number of components, i.e., the light source number ( $M_L$ ) can be determined as discussed in the next section.

### 3.3. Light Source Number Estimation

The problem of determining the number of components in mixture models has been well studied in the statistical learning community [3, 17]. For instance, Cang et al. [2] used the Williams' statistical test to estimate the number of components in mixtures.

Using the notation of [2], Kullback-Leibler divergence distance between the true density function  $p(X)$  and the density function,  $p_k(X)$ , approximated by the EM algorithm under the number,  $k$ , of components is described as:

$$D(p, p_k) = - \int_{-\infty}^{\infty} p(X) \log \frac{p(X)}{p_k(X)} dX$$

$$= - \int_{-\infty}^{\infty} p(X) \log p_k(X) dX + \int_{-\infty}^{\infty} p(X) \log p(X) dX$$

The first term only depends on  $k$  and it is approximated as:

$$\Phi = - \int_{-\infty}^{\infty} p(X) \log p_k(X) dX$$

$$= E_p(-\log p_k(X)) \approx -\frac{1}{N} \sum_{n=1}^N \log p_k(X_n) \quad (12)$$

where  $E_p(\cdot)$  denotes the expectation value function and  $\{X_1, \dots, X_N\}$  is a data set. As  $k$  is increasing,  $\Phi$  has a decreasing trend. Let  $Y_k = -\log p_k(X_n)$ . Then, from (12), the mean,  $\bar{Y}_k$ , of  $Y_k$  represents the mean for different group level in Williams' test. According to Williams' test, statistical significance, i.e., the optimal number of components in a mixture, is determined by the Student's t test using

$$\bar{t}_i = (\hat{M}_{K+1-i} - \hat{M}_K) \left( \frac{2s^2}{N} \right)^{-1/2} \quad (13)$$

where  $\hat{M}_i$  and  $s$  are, respectively, represented as follows:

$$\hat{M}_i = \dots = \hat{M}_j = \min_{j \in [i, K]} \sum_{l=i}^j \frac{\bar{Y}_l}{j-i+1} \quad (14)$$

$$s^2 = \sum_{i=1}^K \sum_{n=1}^N \frac{(Y_{in} - \bar{Y}_i)^2}{\nu} \quad (15)$$

### 3.4. Final Refinement

The estimates obtained in Sections 3.2-3.3 may deviate a little from the true values, since the estimation algorithm is based on the approximated analysis of the Torrance-Sparrow reflection model and illumination sphere. In this section, we improve the results in Sections 3.2-3.3 through an optimization process based on the original Torrance-Sparrow reflection model. Note that we fix the number ( $M_L$ ) and direction ( $\boldsymbol{\mu}_l$ ) of the light sources, since the algorithm described in Sections 3.2-3.3 is, as confirmed by our preliminary experiments, reasonably accurate with respect to these parameters in most cases and because those parameters are difficult to solve stably within the optimization framework.

Using the original (simplified) Torrance-Sparrow model, (8) can be modified as:

$$\mathbf{I}_S \approx I_S \mathbf{L}, \quad I_S = \frac{1}{\cos \theta_r} \sum_{l=1}^{M_L} \tilde{L}_l \exp\left[-\frac{\alpha_l^2}{2\sigma^2}\right] \quad (16)$$

where  $\tilde{L}_l = 2\pi K_S L_l / N_L$ ,  $l = 1, \dots, M_L$ . This implies that estimation of  $K_S$  and  $L_l$  becomes an ill-posed problem. Therefore, we address the estimation of  $\tilde{L}_l$  in (16). The relative source radiance can be calculated by normalizing each  $\tilde{L}_l$  so that  $\sum_{l=1}^{M_L} \tilde{L}_l = 1$ .

Now, we re-estimate  $\tilde{L}_l$  and  $\sigma$  by solving the optimization problem as:

$$\underset{\tilde{\Theta}}{\operatorname{argmin}} \sum_{(s,t)=(0,0)}^{N_S, N_T} |I(s,t) - I_S(s,t)|^2 \quad (17)$$

where  $\tilde{\Theta} = \{\tilde{L}_1, \dots, \tilde{L}_{M_L}, \sigma\}$ ,  $I(s,t)$  is the image irradiance of the observed (separated) specular reflection component, and  $(N_S, N_T)$  is the numbers of horizontal and vertical pixels, respectively. To solve (17), we utilize an iterative approach, as described in the following procedures.

First, we set the initial values of  $\tilde{L}_l$  and  $\sigma$  as:

$$\tilde{L}_l^0 = \gamma^* L_l^*, \quad \sigma^0 = \frac{1}{2\sqrt{\kappa^*}} \quad (18)$$

where  $L_l^*$  and  $\kappa^*$  are the (initial) estimates of  $L_l$  and  $\kappa$  obtained in Sections 3.2-3.3, respectively and  $\gamma^*$  is the solution to the following linear least squares problem:

$$\gamma^* = \underset{\gamma}{\operatorname{argmin}} \sum_{(s,t)=(0,0)}^{N_S, N_T} |I(s,t) - \gamma I_S^*(s,t)|^2 \quad (19)$$

where  $I_S^*$  represents the specular image synthesized using the estimates which we obtained in Sections 3.2-3.3.

Next, we alternate between gradient descent minimization of (17) with respect to  $\tilde{L}_l$  and  $\sigma$  until convergence.



Figure 3. Left: input image, right: specular image.

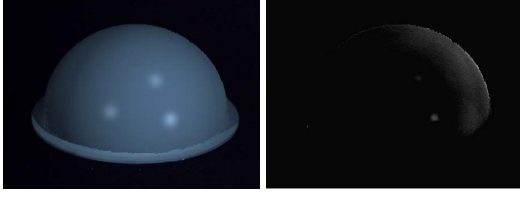


Figure 4. Left: synthesized image, right: difference image (the intensity values are scaled for better visualization).

## 4. Experimental Results

To demonstrate and evaluate our method, we use two examples: a surface with relatively small roughness and one with large roughness. In both experiments, we use a geodesic dome consisting of approximately 4,100 vertices. We search for the optimal number ( $M_L$ ) of light sources in the interval from 1 to 5. Also, we use the acceptance-rejection technique to generate 1000 training data according to the distribution on the illumination sphere (the results were observed to be independent of the seed of the random number generator in our experiment). For each experiment, we also synthesize the object’s appearance under such novel lighting conditions that only one light source is turned on and the others are turned off. In this case, we render the new diffuse image by computing the ratio of irradiance between the original and new lighting condition for each surface point. Then, by synthesizing the new specular image with the estimated illumination and specular parameters, and adding those diffuse and specular images, we can render the virtual object image under the new lighting condition .

First, we describe experimental results with an object with relatively small surface roughness. In this experiment, color images are captured using a color CCD video camera and 3D geometric models are obtained using a light-stripe range finder with a liquid crystal shutter. In our experiments, we use a polarization filter to separate the diffuse and specular reflection components [20]. Note that other techniques, including color-based methods [15], can be used instead. Fig. 3 shows the input image and the specular reflection image. The synthetic image on the left in Fig. 4 has been generated using our method. The right of Fig. 4 shows the difference between the synthetic image and the

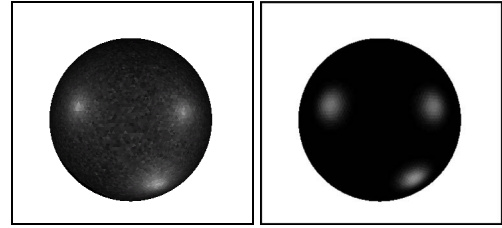


Figure 5. Left: real illumination hemisphere, right: estimated illumination hemisphere.

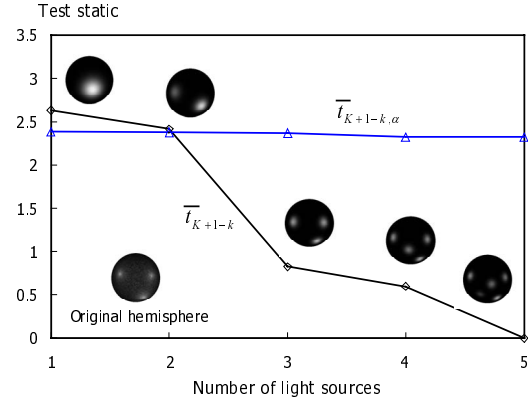


Figure 6. Light source number estimation.

input image (Fig. 4:Left - Fig. 3:Left). Fig. 5 shows the input and finally reconstructed illumination spheres. Fig. 6 shows the process of estimating the number of light sources by decreasing the number of mixture components in the initial estimation. The vertical axis represents the value of the Student’s t-distribution. The horizontal axis represents the setting number of mixture components. In Fig. 6, at the correct number of components  $i = 3$ , the two criteria ( $\bar{t}_i < \bar{t}_{i,\alpha}$  and  $\bar{t}_{i+1} > \bar{t}_{i+1,\alpha}$  : the significance level  $\alpha = 1\%$ ) are simultaneously satisfied and thus the number of light sources can be determined as  $M_L = 3$ . The directions and intensities of light sources are tabulated in Table 1. The estimate of  $\sigma$  is 0.0749. Fig. 7 shows the original photographs and the images rendered under new lighting conditions in which only one light source is turned on.

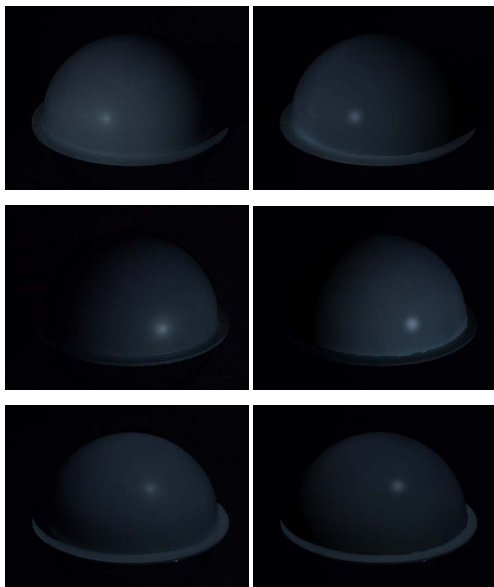
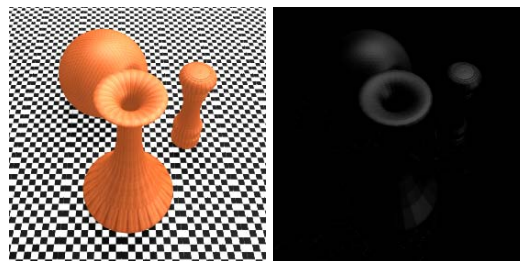
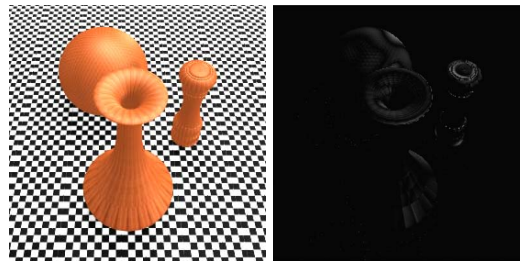
Next, we describe experimental results with objects with relatively large surface roughness values. In this experiment, we synthesize the input image using a global illumination renderer Radiance [11]. Fig. 8 shows the input image and the specular reflection image. The synthetic image on the left in Fig. 9 has been generated using our method. The right of Fig. 9 shows the difference between the synthetic image and the input image (Fig. 9:Left - Fig. 9:Left). Fig. 10 shows the input and the estimated illumination sphere. Fig. 11 shows the process of estimating the number of light sources. From Fig. 11, we can deter-

**Table 1.** Estimation results.

	Light 1	Light 2	Light 3
Estimated light direction	(-0.873, -0.134, 0.470)	(-0.012, -0.962, 0.272)	(0.084, -0.442, 0.893)
Ground truth	(-0.898, -0.119, 0.423)	(-0.0469, -0.978, 0.2)	(0.0379, -0.517, 0.855)
Estimated light intensity	0.291	0.432	0.276
Ground truth	0.276	0.444	0.280

**Table 2.** Estimation results.

	Light 1	Light 2	Light 3	Light 4
Estimated light direction	(0.490, 0.075, -0.868)	(0.551, 0.833, -0.045)	(0.880, 0.168, 0.445)	(0.0373, 0.942, -0.333)
Ground truth	(0.497, 0.109, -0.861)	(0.531, 0.822, -0.204)	(0.861, 0.274, 0.429)	(0.0208, 0.943, -0.333)
Estimated light intensity	0.204	0.294	0.141	0.361
Ground truth	0.2	0.3	0.15	0.35

**Figure 7.** Images under each point light source (left: original photograph, right: synthesized images).**Figure 8.** Left: input image, right: specular image.**Figure 9.** Left: synthesized image, right: difference image (the intensity values are scaled for better visualization).

mine  $M_L = 3$  as the estimated number of light sources. The directions and intensities of light sources are tabulated in Table 2. The estimate of  $\sigma$  is 0.185. Fig. 12 shows the original images and the synthetic images rendered under novel lighting conditions in which only one light source is turned on (Due to the space limitation, we omit the figures for the fourth light). Fig. 12 demonstrates that the estimated light source directions contain errors due to the extremely large surface roughness value.

## 5. Conclusions

We have proposed a new method for estimating the illumination condition of a scene and reflectance property of a real object in the scene, from a single view image taken under multiple point sources and a geometric model of the object. By first representing the specular reflection as a mixture of probability distributions on the unit

sphere and then applying the EM framework to estimate the mixtures, we are able to estimate not only the direction and intensity of the light sources but also the number of light sources and the specular reflectance property. We believe that other reflectance models described with half-angle vector parameterization can be incorporated albeit minor modifications in the derivation. We also believe that multiple images will increase the sampling density of the mixture of vMF distributions and hence increase the accuracy of the estimates. In the future, we would like to extend the presented method to the inverse rendering algorithm to objects that have nonhomogeneous specular reflectance properties. We are also interested in estimating the distance to each source.

## References

- [1] A. Banerjee, I. Dhillon, J. Ghosh, and S. Sra, "Generative model-based clustering of directional data," *Proc. the Ninth ACM SIGKDD Intl. Conf. Knowledge Discovery and Data Mining*, pp.19–28, 2003.

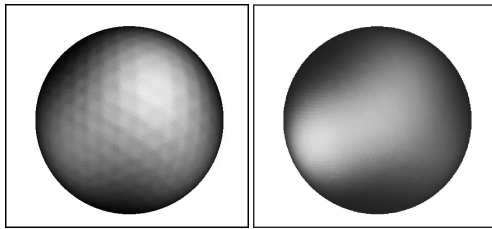


**Figure 10.** Left: real illumination hemisphere, right: estimated illumination hemisphere.

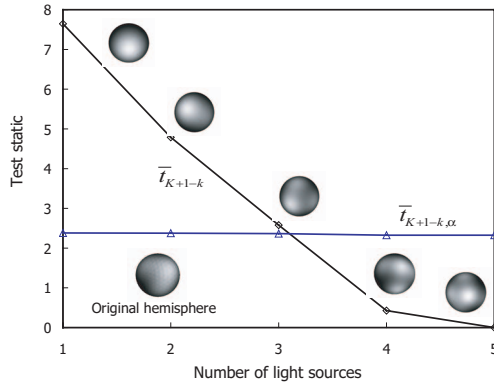


**Figure 11.** Light source number estimation.

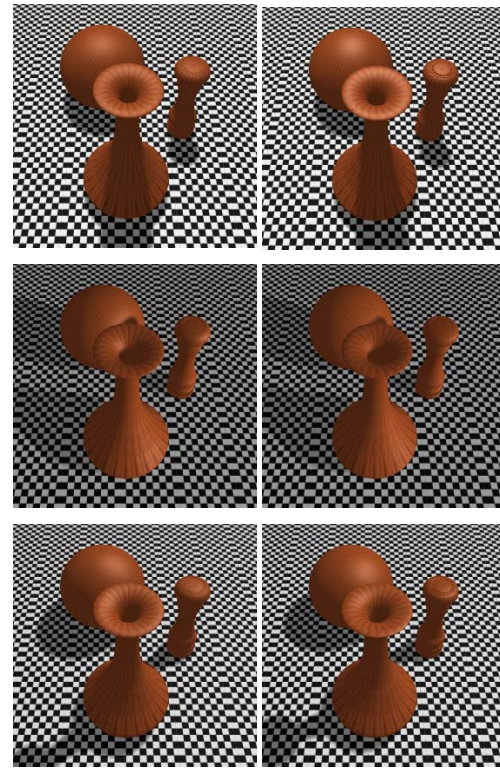


**Figure 12.** Images under each point light source (left:original image, right:synthesized images).

- [2] S. Cang and D. Partridge, “Determining the number of components in mixture models using Williams’ statistical test,” *Proc. 8th Intl. Conf. Neural Information Processing*, pp.14–18, 2003.
- [3] M. Figueiredo and A.K. Jain, “Unsupervised learning of finite mixture models,” *IEEE Trans. Patt. Anal. Mach. Intell.*, **24**(3), pp.381–396, 2002.
- [4] R.A. Fisher, “Dispersion on a sphere,” *Proc. the Royal Society of London Series A 217*, pp.295–305, 1953.
- [5] D.R. Hougen and N. Ahuja, “Estimation of the light source distribution and its use in integrated shape recovery from stereo shading,” *Intl. Conf. Computer Vision*, pp.148–155, 1993.
- [6] K. Ikeuchi and K. Sato, “Determining reflectance properties of an object using range and brightness images,” *IEEE Trans. Patt. Anal. Mach. Intell.*, **13**(11), pp.1139–1153, 1991.
- [7] C-Y. Kim, A.P. Petrov, H-K. Choh, Y-S. Seo, and I-S. Kweon, “Illuminant direction and shape of a bump,” *J. Opt. Soc. Am. A*, **15**(9), pp.2341–2350, 1998.
- [8] Y. Li, S. Lin, H. Lu, and H. Shum, “Multiple-cue illumination estimation in textured scenes,” *Intl. Conf. Computer Vision*, pp.1366–1373, 2003.
- [9] S.R. Marschner and D.P. Greenberg, “Inverse lighting for photography,” *Proc. the Fifth Color Imaging Conference*. Society for Imaging Science and Technology, pp.262–265, 1997.
- [10] K. Nishino, *Photometric Object Modeling –Rendering from a Dense/Sparse Set of Images–*, Ph.D. Thesis, Graduate School of Science, The University of Tokyo, 2002.
- [11] <http://radsite.lbl.gov/radiance/HOME.html>, 1997.
- [12] R. Ramamoorthi and P. Hanrahan, “A signal processing framework for inverse rendering,” *Proceedings of SIGGRAPH*, pp.117–128, 2001.
- [13] I. Sato, Y. Sato, and K. Ikeuchi, “Illumination from shadows,” *IEEE Trans. Patt. Anal. Mach. Intell.*, **25**(3), pp.290–300, 2003.
- [14] F. Solomon and K. Ikeuchi, “Extracting the shape and roughness of specular lobe objects using four light photometric stereo,” *Intl. Conf. Computer Vision and Pattern Recognition*, pp.466–471, 1992.
- [15] R.T. Tan and K. Ikeuchi, “Separating reflection components of textured surfaces from a single image,” *IEEE Trans. Patt. Anal. Mach. Intell.*, **27**(2), pp.178–193, 2005.
- [16] K.E. Torrance and E.M. Sparrow, “Theory of off-specular reflection from roughened surfaces,” *J. Opt. Soc. Am. A*, **57**, pp.1105–1114, 1967.
- [17] J. Verbeek, N. Vlassis, and B. Krose, “Efficient greedy learning of gaussian mixture models,” *Neural Computation*, **15**(2), pp.469–485, 2003.
- [18] Y. Wang and D. Samaras, “Estimation of multiple illuminants from a single image of arbitrary known geometry,” *Proc. European Conference on Computer Vision*, pp.272–288, 2002.
- [19] Y. Wang and D. Samaras, “Estimation of multiple directional light sources for synthesis of augmented reality images,” *Graphical Models*, **65**(4), pp.185–205, 2003.
- [20] L.B. Wolff and T.E. Boult, “Constraining object features using a polarization reflectance model,” *IEEE Trans. Patt. Anal. Mach. Intell.*, **13**(6), pp.167–189, 1991.
- [21] Y. Yang and A. Yuille, “Source from shading,” *Proc. IEEE Computer Vision and Pattern Recognition*, pp.534–539, 1991.
- [22] Y. Zhang and Y.H. Yang, “Multiple illuminant direction detection with application to image synthesis,” *IEEE Trans. Patt. Anal. Mach. Intell.*, **23**(8), pp.915–920, 2001.
- [23] Q. Zheng and R. Chellappa, “Estimation of illuminant direction, albedo, and shape from shading,” *IEEE Trans. Patt. Anal. Mach. Intell.*, **13**(7), pp.680–702, 1991.